JOURNAL OF GUIDANCE, CONTROL, AND DYNAMICS
Vol. 24, No. 5, September–October 2001

Robust Output Feedback Using Sliding Mode Control

A. S. Lewis*
Pennsylvania State University, State College, Pennsylvania 16804

A general sliding mode output feedback algorithm is developed that takes into account parametric uncertainty and external disturbances provided certain bounds are known. It has been assumed that the number of states is greater than the number of sensors and that there can be a mismatched disturbance. The details of an eigenvalue perturbation analysis for an uncertain matrix are presented. A boundary layer has been introduced around each sliding surface to eliminate the chattering phenomenon. The results from numerical simulations are presented to corroborate the validity of the proposed controller.

Introduction

IN the context of robust control, it is well known that sliding mode controllers can be designed to account for parametric error, external disturbances, and system uncertainty provided that certain bounds are known. This is especially true when all of the states of the system are accessible for measurement. However, full state feedback is generally not possible or feasible, and reliance on only a few outputs is necessary. One example of such a system is a flexible rotor where the excitation is caused by the inevitable uncertainties in the rotor eccentricity. Although it is not possible to know the exact value of the rotor eccentricity, it is quite a straightforward task to estimate its maximum value. Another example concerns the active control of a truck/full-trailer's rearward amplification during lane changes and braking. During these maneuvers, it is generally impossible to measure all of the states, and certain parameters such as the tire's cornering stiffness and articulation angle are not known exactly but can be bounded. As a result, it is important to develop the sliding mode controller based on a limited number of inputs and to ensure that robustness to external disturbances and parametric uncertainty is guaranteed.

Yallapragada et al.[1] discuss a design method to obtain a controller that satisfies the reaching conditions. They also examine the robustness to external disturbances when the matching conditions are met. Wang and Fan[2] have developed an interesting approach to design a sliding mode output feedback control. Their definition of sliding hyperplanes includes an exponentially decaying term. Effectively, the system starts from being initially on the sliding hyperplanes. However, they did not address the issue of robustness to external disturbances. Kwan[3] extended the approach by Wang and Fan[2] by eliminating the exponentially decaying term and formulating a time-varying upperbound of states. He has also examined the robustness to mismatched disturbances. However, this disturbance vector has a special structure that may limit its applicability to many systems. Furthermore, he does not consider uncertainty in the control matrix. Lewis et al.[4] apply sliding mode output feedback to control a flexible rotor with uncertainty in the external disturbance and initial conditions. Lewis and Sinha[5] address the mismatched disturbance issue concerned with output feedback and present techniques for stability analysis. However, in the latter two efforts, parametric uncertainty is not considered.

This paper develops a general sliding mode output feedback control methodology that addresses uncertainty in the plant, control, and disturbance matrices provided certain bounds are known. It is assumed that the number of states is greater than the number of sensors. The robustness to the parametric uncertainty and external disturbances is achieved through the proper selection of control gains. The method for determining these gains is given, as well as a breakdown of the components that contribute to the magnitude of these gains. Using a two-degree-of-freedom spring–mass–damper system (Fig. 1) and an aircraft model, simulation results with both matched and mismatched disturbances are presented that illustrate the controller design procedure and the effectiveness of the controller as well.

Problem Statement

Consider the following general system:

$$\dot{\boldsymbol{x}} = (A + \Delta A)\boldsymbol{x} + (\hat{B} + \Delta\hat{B})\boldsymbol{u} + (D + \Delta D)\boldsymbol{F}_d \tag{1}$$

$$\boldsymbol{Y} = Cx \tag{2}$$

where $\boldsymbol{x} \in R^n$ is the state vector, $\boldsymbol{u} \in R^m$ is the control vector, and $\boldsymbol{Y} \in R^p$ is the output measurement vector. The matrices ΔA, $\Delta\hat{B}$, and ΔD account for parametric uncertainty in the plant, control, and disturbance matrices, respectively. The disturbance $\boldsymbol{F}_d$ is assumed to be bounded and $C \in R^{p\times n}$ is the output matrix. It is assumed that the matching condition as outlined by Verghese et al.[6] is satisfied for the control matrix, that is, $\Delta\hat{B} = \Delta B\hat{B}$, where ΔB is a bounded matrix and $B = (I + \Delta B)\hat{B} = \hat{B}$ in the absence of uncertainty. The objective is to use sliding mode output feedback to regulate the output in the presence of uncertainty. The system is converted to controllable canonical form given by Dorling and Zinober[7] by introducing the transformation

$$\boldsymbol{q} = T\boldsymbol{x} \tag{3}$$

with $T = T^T$. The transformed equations with $\boldsymbol{q}^T = [\boldsymbol{q}_1^T \;\; \boldsymbol{q}_2^T]$, $\boldsymbol{q}_1 \in R^{n-m}$ and $\boldsymbol{q}_2 \in R^m$, are

$$\dot{\boldsymbol{q}}_1 = (A_{11} + \Delta A_{11})\boldsymbol{q}_1 + (A_{12} + \Delta A_{12})\boldsymbol{q}_2 + (D_1 + \Delta D_1)F_d \tag{4}$$

$$\dot{\boldsymbol{q}}_2 = (A_{21} + \Delta A_{21})\boldsymbol{q}_1 + (A_{22} + \Delta A_{22})\boldsymbol{q}_2 + (I + \Delta B_2)\hat{B}_2\boldsymbol{u} + (D_2 + \Delta D_2)\boldsymbol{F}_d \tag{5}$$

$$\boldsymbol{Y} = CT^T\boldsymbol{q} = C_1\boldsymbol{q}_1 + C_2\mathbf{q}_2 \tag{6}$$

where C_1 and C_2 are appropriately defined matrices.

Control Law Development

The sliding hyperplanes are introduced as

$$S = (GC_2)^{-1}G\boldsymbol{Y} = (GC_2)^{-1}GC_1\boldsymbol{q}_1 + \boldsymbol{q}_2 \tag{7}$$

where $\boldsymbol{S} \in R^m$ and (GC_2) is assumed to be invertible. The matrix $G \in R^{m\times p}$ is selected by the designer. Equation (7) can be rewritten to express $\boldsymbol{q}_2$ in terms of $\boldsymbol{q}_1$ and $\boldsymbol{S}$ as

$$\boldsymbol{q}_2 = \boldsymbol{S} - (GC_2)^{-1}GC_1\boldsymbol{q}_1 \tag{8}$$

Received 20 March 2000; revision received 10 October 2000; accepted for publication 5 January 2001.

*Research Associate, Applied Research Laboratory, Autonomous Control and Intelligent Systems.

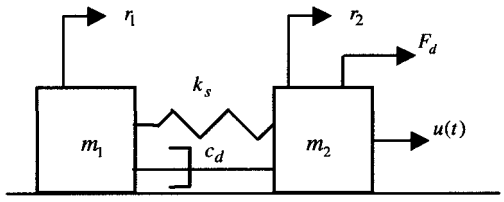

Fig. 1 Two-degree-of-freedom system.

Substituting Eq. (8) into Eq. (4) gives

$$\dot{q}_1 = A_{\text{red}}\boldsymbol{q}_1 + (A_{12} + \Delta A_{12})\boldsymbol{S} + (D_1 + \Delta D_1)\boldsymbol{F}_d \tag{9}$$

$$A_{\text{red}} = A_{11} - A_{12}(GC_2)^{-1}GC_1 + \Delta A_{11} - \Delta A_{12}(GC_2)^{-1}GC_1 \tag{10}$$

where G must be chosen to ensure that the eigenvalues of the reduced-order matrix A_{red} are stable. A_{red} has uncertainties associated with it, but they are assumed to be bounded. It is known that in the absence of uncertainty, arbitrary pole placement is possible[2] if

$$\text{rank}\left[C_2(GC_2)^{-1}G - 1\right] \leq p - m \tag{11}$$

If this condition is not satisfied, it still may be possible to achieve stable poles even in the presence of uncertainty, but they may not be arbitrary. Wilkinson[8] discusses eigenvalue perturbation theory based on theorems from Gerschgorin. The main premise is that every eigenvalue of a given matrix must lie in at least one circular disk with given center and radius. Smith et al.[9] use an approach involving eigenvalue perturbation descriptions to design H_∞ controllers for flexible structure problems. Weigl et al.[10] also apply H_∞ control with eigenvalue perturbations to stabilize a transonic compressor. Finally, Smith[11] presents perturbation models for robust control where the matrices are perturbed by a set of all unknown, Euclidean norm-bounded matrices. These methods can be applied to matrices that have both complex and/or real eigenvalues. The key to the application is casting the system matrix as the sum of a nominal matrix and a perturbed matrix multiplied by a diagonal weighting matrix. The elements of this weighting matrix are the radii of the circular disks within which the eigenvalues must lie.

With a stable A_{red} matrix having been determined, the eigenvalues of A_{red} can be grouped as $[-\lambda_1 \;\; -\lambda_2 \;\; \cdots \;\; -\lambda_{n-m}]$. Kwan[3] shows that

$$\|\exp(A_{\text{red}}t)\| \leq \gamma \exp(-\lambda_{\min}t) \tag{12}$$

where $\lambda_{\min} > 0$ is the minimum real part of the λ_i and $\lambda > 0$. Thus, the important issue with this design is being able to determine $\lambda_{\min}$ given a stable set of eigenvalues.

With a properly designed sliding mode control system, the outputs reach a desired manifold (intersection of sliding hyperplanes) and stay on the manifold thereafter. These two stages are referred to as the reaching and sliding conditions, respectively. While in the sliding mode, the system dynamics can be written as $\dot{S} = 0$. Differentiating Eq. (7) and using Eqs. (5), (8), and (9) yield

$$\dot{S} = P\boldsymbol{q}_1 + Q\boldsymbol{S} + RF_d + (I + \Delta B_2)\hat{B}_2\boldsymbol{u} \tag{13}$$

where

$$P = (GC_2)^{-1}GC_1\left[A_{11} + \Delta A_{11} - (A_{12} + \Delta A_{12})(GC_2)^{-1}GC_1\right] + A_{21} + \Delta A_{21} - (A_{22} + \Delta A_{22})(GC_2)^{-1}GC_1 \tag{14}$$

$$Q = (GC_2)^{-1}GC_1(A_{12} + \Delta A_{12}) + (A_{22} + \Delta A_{22}) \tag{15}$$

$$R = (GC_2)^{-1}GC_1(D_1 + \Delta D_1) + (D_2 + \Delta D_2) \tag{16}$$

Because the system dynamics are not known exactly, the best estimate of the control $\boldsymbol{u}$ that makes $\dot{S} = 0$ is required. To satisfy $\dot{S} = 0$ as closely as possible and to account for the uncertainties in the system, let the control law take the form

$$\boldsymbol{u} = -\hat{B}_2^{-1}K\bar{\boldsymbol{S}} \tag{17}$$

where

$$K = \text{diag}(k_1, k_2, \ldots, k_m) \tag{18}$$

$$\bar{\boldsymbol{S}} = [\text{sign}(s_1), \text{sign}(s_2), \ldots, \text{sign}(s_m)]^T \tag{19}$$

Substitution of Eq. (17) into Eq. (13) yields

$$\dot{S} = P\boldsymbol{q}_1 + Q\boldsymbol{S} + RF_d - (I + \Delta B_2)K\bar{S} \tag{20}$$

The reaching conditions, $s_i\dot{s}_i \leq -\eta_i|s|$, are satisfied if

$$(I - E)K = \|P\boldsymbol{q}_1\| + \|Q\|\|\boldsymbol{S}\| + \|R\boldsymbol{F}_d\| \tag{21}$$

where $|\Delta B_2| \leq E$, $\|\bullet\|$ is the 2-norm of a vector, and $|\bullet|$ indicates that every element is considered to be greater than or equal to zero. Equation (21) is a set of m equations with m unknown gains K to be determined. It is of interest to know if there is a unique solution for K, and if so, is every component of $K > 0$? Slotine and Li[12] show by the theorem of Frobenius–Perron that Eq. (21) admits a unique solution for K whose components are nonnegative.

By the use of Eq. (12), the norm of $\boldsymbol{q}_1$ can be expressed as

$$\|\boldsymbol{q}_1(t)\| \leq \gamma e^{-\lambda_{\min}t}\|\boldsymbol{q}_1(0)\| + \int_0^t \gamma e^{-\lambda_{\min}(t-\tau)}\left[\|(A_{12} + \Delta A_{12})\|\|\boldsymbol{S}\| + d^*\right]\mathrm{d}\tau \tag{22}$$

with $\|(D_1 + \Delta D_1)\boldsymbol{F}_d(t)\| < d^*$. However, the vector $\boldsymbol{q}_1$ is not available for measurement. To circumvent this problem, an auxiliary variable is introduced similarly to that of Kwan,[3] who does not consider the ΔA_{12} matrix in his formulation, as

$$\dot{w}(t) = -\lambda_w(t) + \gamma\left[\|(A_{12} + \Delta A_{12})\|\|\boldsymbol{S}\| + d^*\right] \tag{23}$$

with $w(0) > 0$, and $\lambda_w < \lambda_{\min}$. Integration of Eq. (23) yields

$$w(t) = e^{-\lambda_w t}w(0) + \int_0^t \gamma e^{-\lambda_w(t-\tau)}\left[\|(A_{12} + \Delta A_{12})\|\boldsymbol{S}\| + d^*\right]\mathrm{d}\tau \tag{24}$$

Comparison of Eqs. (22) and (24) indicates that $w(t) \geq \|\boldsymbol{q}_1(t)\|$ after a finite period of time. As a result, the gains K_i can be expressed as

$$\boldsymbol{K} = (I - E)^{-1}[\|P\|w(t) + \|Q\|\|\boldsymbol{S}\| + \|R\|\|\boldsymbol{F}_d\|] \tag{25}$$

Inspection of Eq. (25) indicates that K is time varying due to the $w(t)$ and S terms. To eliminate the chattering phenomenon, the sign function of Eq. (19) is replaced by the saturation function defined as

$$\text{sat}\left[\frac{s_i(t)}{\phi_i(t)}\right] = \begin{cases} s_i(t)/\phi_i(t); & \text{if} \quad |s_i(t)/\phi_i(t)| < 1 \\ \text{sign}[s_i(t)/\phi_i(t)]; & \text{otherwise} \end{cases} \tag{26}$$

In essence, a boundary layer[12] is introduced around each sliding hyperplane so that the control is a nonlinear function of the inputs outside the boundary layer and a linear function inside the boundary layer.

Example 1

To demonstrate the control technique, the two-degree-of-freedom mechanical system shown in Fig. 1 will be used for example 1, and an aircraft application will be presented in example 2. It is assumed that only r_2 and $\dot{r}_2$ are available for measurement. Here $u(t)$ is the control force, and $F_d(t)$ is the disturbance force. When the disturbance force is acting on the right mass of Fig. 1, the matching condition is met. To simulate the nonmatching condition, $F_d(t)$ is taken to be acting on

the left mass. The equations of motion, when $F_d(t)$ is applied to the right mass, can be put into first-order form after Eqs. (4) and (5) as

$$\boldsymbol{q}_1 = [r_1 \quad r_2 \quad \dot{r}_1]^T, \qquad \boldsymbol{q}_2 = [\dot{r}_2] \tag{27}$$

$$A_{11} + \Delta A_{11} = \begin{bmatrix} 0 & 0 & 1 \\ 0 & 0 & 0 \\ -k_s/m_1 - \alpha_1 & k_s/m_1 + \alpha_1 & -c_d/m_1 - \alpha_3 \end{bmatrix} \tag{28}$$

$$A_{12} + \Delta A_{12} = [0 \quad 1 \quad c_d/m_1 + \alpha_3]^T \tag{29}$$

$$A_{21} + \Delta A_{21} = [k_s/m_2 + \alpha_2 \quad -k_s/m_2 - \alpha_2 \quad c_d/m_2 + \alpha_4] \tag{30}$$

$$A_{22} + \Delta A_{22} = [-c_d/m_2 - \alpha_4], \qquad \hat{B}_2 = [1/m_2]$$

$$\Delta B_2 = [\alpha_5] \tag{31}$$

$$D_1 + \Delta D_1 = [0 \quad 0 \quad 0]^T, \qquad D_2 + \Delta D_2 = [(1/m_2) + \alpha_5] \tag{32}$$

$$C_1 = \begin{bmatrix} 0 & 1 & 0 \\ 0 & 0 & 0 \end{bmatrix}, \qquad C_2 = \begin{bmatrix} 0 \\ 1 \end{bmatrix} \tag{33}$$

where

$$\alpha_1 = e_1(1 + \cos 5t), \qquad \alpha_2 = e_2 \cos 3t, \qquad \alpha_3 = e_3 + e_4 \sin 2t \tag{34}$$

$$\alpha_4 = e_5 + e_6 \sin 2t, \qquad \alpha_5 = e_7(1 - \sin t \cos 3t) \tag{35}$$

When the matching conditions for the disturbance force are not met, that is, the force is acting on the left mass, the disturbance matrices are defined as

$$D_1 + \Delta D_1 = [0 \quad 0 \quad 1/m_1 + \alpha_5]^T, \qquad D_2 + \Delta D_2 = [0] \tag{36}$$

Let the disturbance force be described by

$$F_d(t) = A_0 \cos \Omega t \tag{37}$$

where A_0 is the magnitude of the disturbance. The parameters for the system model are given as $m_1 = 5$ kg, $m_2 = 4$ kg, $c_d = 7$ Ns/m, and $k_s = 500$ N/m. The simulation parameters are $\Omega = 14.137$ rad/s, $e_1 = 11.0$, $e_2 = 15$, $e_3 = 0.25$, $e_4 = 0.25$, $e_5 = 1.0$, $e_6 = 1.0$, and $e_7 = 0.1$. The magnitude of the uncertainties is based on the physical parameters of the system, and it is assumed that this magnitude does not exceed the nominal value. The frequencies were chosen arbitrarily and were intended to create a time-varying uncertainty. It is assumed that $|\boldsymbol{q}_1(0)| \leq [0.2\text{ m} \quad 0.1\text{ m} \quad 0.1\text{ m/s}]^T$ and that $A_0 \leq 25$ N. It is noted that the uncertainties can lead to parameter variations greater than 20% from the nominal for stiffness, damping, and control matrix terms. In particular, these uncertainties lead to perturbations in the eigenvalues of A_{red}.

Eigenvalue Analysis for Example 1

To run the simulations, a stable A_{red} matrix, given by

$$A_{\text{red}} = \begin{bmatrix} 0 & 0 & 1 \\ 0 & \dfrac{-g_1}{g_2} & 0 \\ \dfrac{k_s}{m_1} + \alpha_1 & \dfrac{-k_s}{m_1} + \dfrac{c_d g_1}{m_1 g_2} - \alpha_1 + \dfrac{\alpha_3 g_1}{g_2} & \dfrac{-c_d}{m_1} - \alpha_3 \end{bmatrix} \tag{38}$$

had to be formed, where $G = [g_1 \quad g_2]$. For the simulations, the matrix G was given by [10 1]. The eigenvalues of the nominal A_{red} matrix are -10.00, $-0.70 \pm i9.9755$. According to the theory given by Smith,[11] $A_{\text{red}} = A_{\text{nom}} + A_{\text{pert}}$ can be rewritten as

$$A_{\text{red}} = A^* + W\Delta \tag{39}$$

where $A^* = Z^{-1} A_{\text{nom}} Z$ has a special structure containing the eigenvalues of the nominal A_{red}, $W\Delta = Z^{-1} A_{\text{pert}} Z$, and W is a diagonal weighting matrix selected such that the largest singular value of $\Delta \leq 1$. The matrix Z is given by $\boldsymbol{V}\boldsymbol{V}_1^{-1}$ where $\boldsymbol{V}$ is the eigenvector matrix for A_{nom} and $\boldsymbol{V}_1$ is the eigenvector matrix for A^*. For the numerical example presented here, which results in the largest singular value for Δ being $0.9926 \leq 1$,

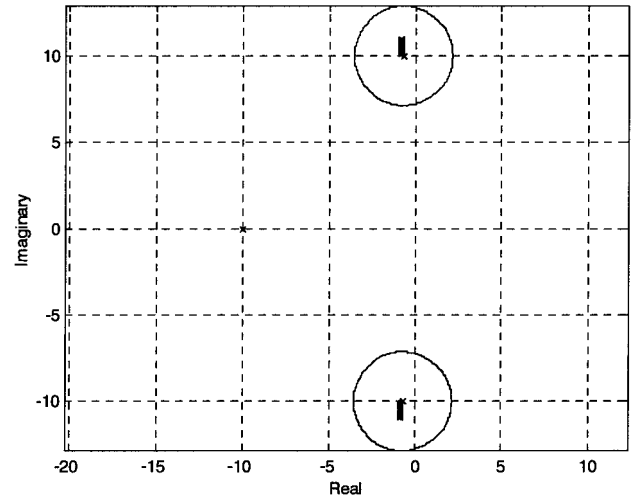

Fig. 2 Eigenvalue perturbation analysis for A_{red}.

$$A^* = \begin{bmatrix} -0.70 & 9.9755 & 0 \\ -9.9755 & -0.70 & 0 \\ 0 & 0 & -10.00 \end{bmatrix}$$

$$W = \begin{bmatrix} 2.85 & 0 & 0 \\ 0 & 2.85 & 0 \\ 0 & 0 & 0.05 \end{bmatrix} \tag{40}$$

Figure 2 shows the interpretation of the A^* and W matrices with regard to the perturbation of the nominal eigenvalues. There are three disks, each with its center at a nominal eigenvalue and each with a radius corresponding to the diagonal elements of W. Inspection of Fig. 2 indicates that the disks encompass areas that may contain unstable eigenvalues. The dark portions inside the two large circles contain the actual range of the possible eigenvalues of A_{red} given in closed form as

$$\lambda_{1,2} = -\tfrac{1}{2}(c_d/m_1 + \alpha_3) \pm j\tfrac{1}{2}\sqrt{(c_d/m_1 + \alpha_3)^2 - 4(k_s/m_1 + \alpha_1)} \tag{41}$$

$$\lambda_3 = -g_1/g_2 \tag{42}$$

It is observed that λ_3 is fixed and has no dependence on the parametric uncertainties. As a result, to keep each element of $W > 0$, a small radius of 0.05 is chosen. In contrast, the minimum real value of $\lambda_{1,2}$, $-(c_d/m_1 + e_3 + e_4)/2 = -0.90$, and the maximum real value, $-c_d/(2m_1) = -0.70$, are time varying as a result of uncertainty. Consequently, if g_1 and g_2 are chosen such that $\lambda_3 < 0$, the A_{red} matrix will always contain stable eigenvalues. As a result, $\lambda_w = 0.40 < 0.70$ satisfies the condition imposed with Eq. (23) and is used in the simulations. It is clear that the approach given by Smith[11] is conservative, but does provide a good bound of the range of the eigenvalues.

Simulation Results for Example 1

Figure 3 shows a plot of $\boldsymbol{y}_1(t) = r_2(t)$ vs time for both the matching and nonmatching conditions. There is a higher amplitude of oscillation for the matched case because the force is acting directly on it. Figure 4 shows a plot of the sliding surface $S(t)$ vs time. In steady-state, it oscillates around zero with frequency Ω. The value of ϕ for both the matching and nonmatching cases is 0.25. It is found that the system remains inside the boundary layer after 0.045 s for the matching case and 0.072 s for the nonmatching case. Inspection of Fig. 5 clearly shows a large difference between the gains K for

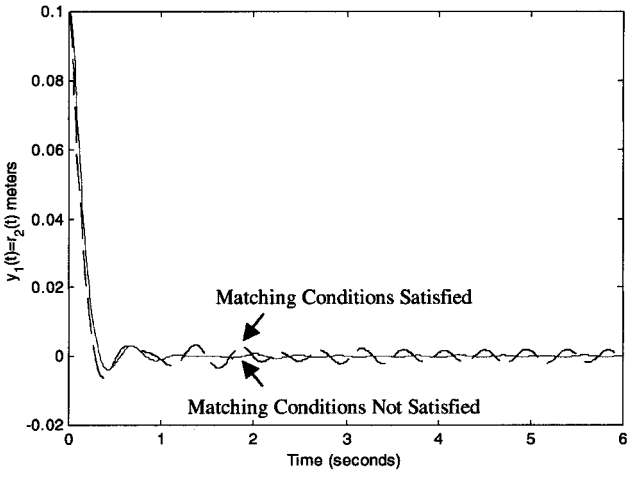

Fig. 3 Plot of $y_1(t)$ vs time.

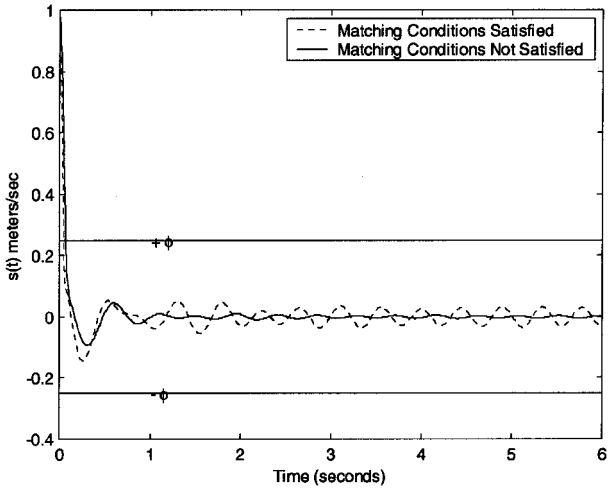

Fig. 4 $S(t)$ vs time.

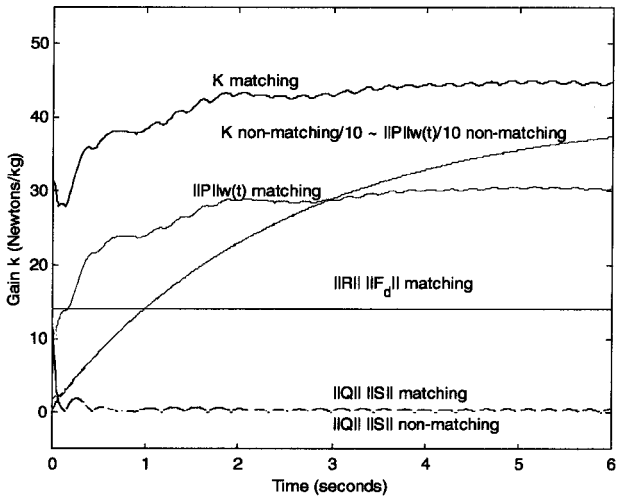

Fig. 5 K vs time.

the two cases indicated by the $\|P\|w(t)$ term being divided by 10. However, there is not a large difference in the overall control effort as shown in Fig. 6. The gain defined by Eq. (25) is composed primarily of the $\|P\|w(t)$ term for both cases, especially for the nonmatching case. The $\|Q\|\|S\|$ term contributes very little to the overall gain. The nonmatching case has no contribution by the $\|R\|\|F_d\|$ term, whereas the matching case has a constant component.

Figure 7 shows how $w(t)$ follows $\|q_1(t)\|$ for both the matching and nonmatching conditions. In each case, $w(0) = 0.01$, but the values for γ are different. The initial condition is selected to be relatively small because the initial conditions of $\boldsymbol{q}$ are not known

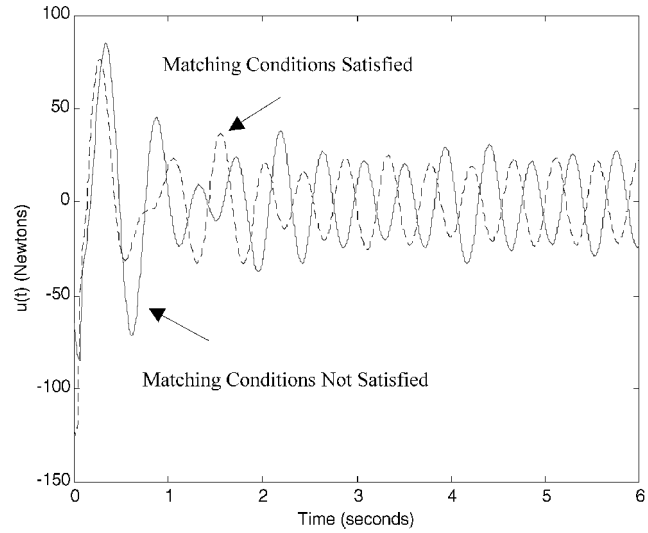

Fig. 6 Two cases, $u(t)$ vs time.

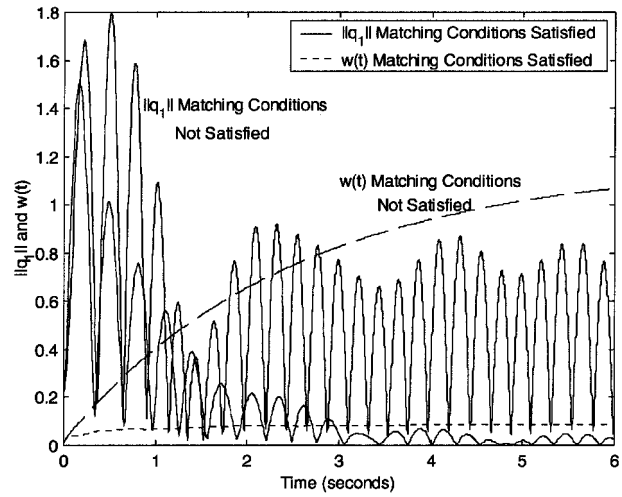

Fig. 7 Two cases, $\|q_1\|$ and $w(t)$ vs time.

exactly. The value of γ directly affects the magnitude of $w(t)$. As seen from Fig. 7, the $\|\boldsymbol{q}_1(t)\|$ for the nonmatching case has a much higher amplitude than the matching case. However, $\gamma_{\text{match}} = 0.4$ while $\gamma_{\text{nonmatch}} = 0.09$. The higher amplitude is needed for the matching case to ensure that $w(t) > \|q_1(t)\|$ in a reasonable time. It is noted that in both cases that $w(t) > \|q_1(t)\|$ at about the 3-s mark. This time could be reduced with larger values of γ, but it would be at the expense of larger control effort. As a result, a design compromise must be found between these two factors.

Example 2

In this aerospace application, adapted from Ref. 13, a linearized model of the longitudinal dynamics of an aircraft is explored and is representative of an aircraft under trim conditions. Both matched and mismatched disturbances are included. The system is given as

$$\begin{bmatrix} \dot{\alpha} \\ \dot{q}_p \\ \dot{\delta}_e \end{bmatrix} = \begin{bmatrix} Z_\alpha/V + \alpha_1 & 1 & Z_E/V + \alpha_4 \\ M_\alpha + \alpha_2 & M_q + \alpha_3 & M_E + \alpha_5 \\ 0 & 0 & -T_e - \alpha_6 \end{bmatrix} \begin{bmatrix} \alpha \\ q_p \\ \delta_e \end{bmatrix} + \begin{bmatrix} 0 \\ 0 \\ T_e + \alpha_7 \end{bmatrix} u + \begin{bmatrix} d_1 \\ d_2 \\ d_3 \end{bmatrix} d(t) \tag{43}$$

where Z_α/V, Z_E/V, M_α, M_q, and M_E are aircraft properties. The angle of attack is α, the pitch rate is q_p, the elevator angle is δ_e, and the dynamics associated with the elevator angle to the control input u is given by T_e. The disturbance is given by $d(t)$, and the values of d_1, d_2, and d_3 determine whether the system has a matched or

mismatched disturbance. The outputs are selected to be the pitch rate and elevator angle. It is noted that by choosing the elevator angle, there is collocation of the sensor and actuator. Finally, α_i represent the uncertainty of the system and are given by

$$\alpha_1 = e_1 \sin t, \qquad \alpha_2 = e_2 \cos 2t, \qquad \alpha_3 = e_3(1 + \cos 5t)$$

$$\alpha_4 = e_4 \cos t \tag{44}$$

$$\alpha_5 = e_5(1 - \sin t), \qquad \alpha_6 = e_6(-1 + \sin 2t \cos t)$$

$$\alpha_7 = e_7 \cos 3t \tag{45}$$

When $e_1 = 0.05$, $e_2 = 2.0$, $e_3 = 0.05$, $e_4 = 0.00005$, $e_5 = 2.0$, $e_6 = 0.667$, and $e_7 = 0.4$ and the parameters given in Ref. 13 are used, the system, given in the form of Eqs. (4–6), is

$$A_{11} + \Delta A_{11} = \begin{bmatrix} -0.277 + 0.05 \sin t & 1 \\ -17.1 + 2 \cos 2t & -0.178 + 0.05(1 + \cos 5t) \end{bmatrix} \tag{46}$$

$$A_{12} + \Delta A_{12} = \begin{bmatrix} -0.0002 \\ -12.2 + 2(1 - \sin t) \end{bmatrix} \tag{47}$$

$$A_{21} + \Delta A_{21} = [0 \quad 0]$$

$$A_{22} + \Delta A_{22} = [-6.67 - 0.667(-1 + \sin 2t \cos t)] \tag{48}$$

$$\hat{B}_2 + \Delta B_2 \hat{B}_2 = [6.67 + 0.4(-1 + \sin 2t \cos t)]$$

$$C_1 = \begin{bmatrix} 0 & 1 \\ 0 & 0 \end{bmatrix}, \qquad C_2 = \begin{bmatrix} 0 \\ 1 \end{bmatrix} \tag{49}$$

It is observed that these uncertainties can lead to parameter variations greater than 20% from the nominal values and give a good indication of the perturbations that might occur during trim conditions. The A_{red} matrix is formed as

$$A_{\text{red}} = \begin{bmatrix} Z_\alpha / V + \alpha_1 & 1 - (Z_E / V + \alpha_4) g_1 / g_2 \\ M_\alpha + \alpha_2 & M_q + \alpha_3 - (M_E + \alpha_5) g_1 / g_2 \end{bmatrix} \tag{50}$$

where $G = [g_1 \;\; g_2]$. For the simulations, the matrix G was given by $[-0.4635 \;\; 1]$, which results in the eigenvalues of the nominal A_{red} matrix being $-3.0549 \pm j3.063$. These nominal eigenvalues are the centers of the stability disks, shown by the x in Fig. 8. Figure 8, which shows the perturbation analysis for A_{red}, indicates that there is no unstable region. Only one circle is shown because the roots appear in complex conjugate pairs. The absence of an unstable region is further demonstrated by the computation of the A^* and W matrices given by

$$A^* = \begin{bmatrix} -3.0549 & 3.063 \\ -3.063 & -3.0549 \end{bmatrix}, \qquad W = \begin{bmatrix} 2.25 & 0 \\ 0 & 2.25 \end{bmatrix} \tag{51}$$

In this case, the largest singular value for the Δ matrix is 0.9910. Inspection of the W matrix indicates the radius is 2.25, which is not large enough to cause the nominal eigenvalues to go outside of the stability disk.

Two cases for simulation are considered: one with a matched disturbance and one with a mismatched disturbance. To obtain a mismatched disturbance, the values of d_1, d_2, and d_3 are taken to be 0.0, 1.0, and 0.0, respectively with constant disturbance $d(t) = 0.5$ after 0.5 s, which is in contrast to the sinusoidal disturbance of example 1. A matched disturbance can be achieved by setting d_1, d_2, and d_3 to 0.0, 0.0, and 1.0, respectively. Control laws for the two types of disturbances can be computed as follows:

$$u_{\text{match}}(t) = -[10.76w(t) + 1.26\|S\| + 0.38]\text{sat}(S/\phi) \tag{52}$$

$$u_{\text{nonmatch}}(t) = -[10.76w(t) + 1.26\|S\| + 0.17]\text{sat}(S/\phi) \tag{53}$$

Simulation results are obtained with $\phi = 0.3$, $\gamma = 1.5$, $\lambda_w = 2$, and $d^* = 0$ for matching and 0.6 for nonmatching, and an initial condition vector of $[0 \;\; -2 \;\; 0]$. The initial value of $w(t)$ is 0.01. Figure 9 shows the response of the attack angle and pitch rate for the two cases, and Fig. 10 shows the control force required in each case. Inspection of Figs. 9 and 10 indicates that the control input required

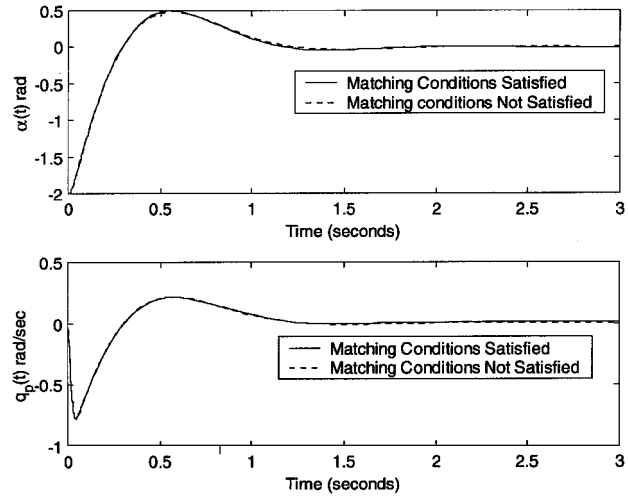

Fig. 9 Aerospace example, $\alpha(t)$ and $q_p(t)$ vs time.

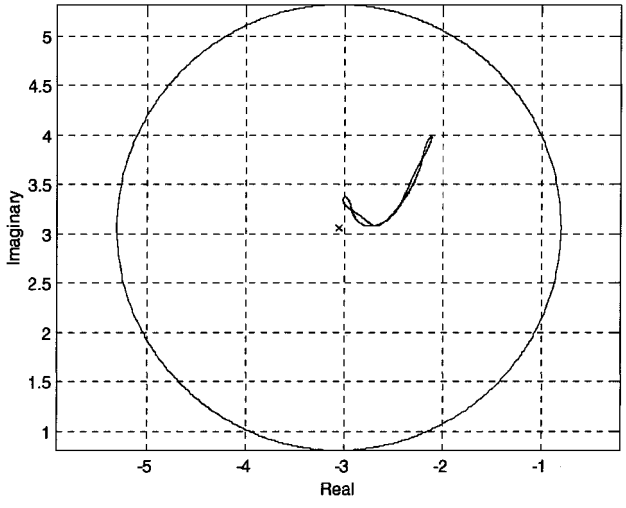

Fig. 8 Eigenvalue analysis for aerospace application.

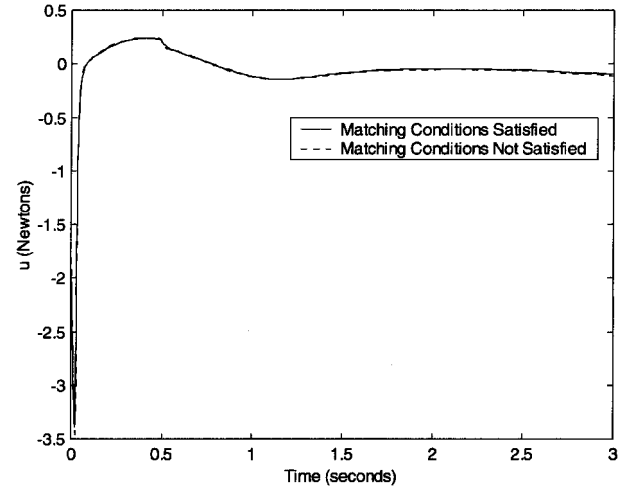

Fig. 10 Aerospace example, $u(t)$ vs time.

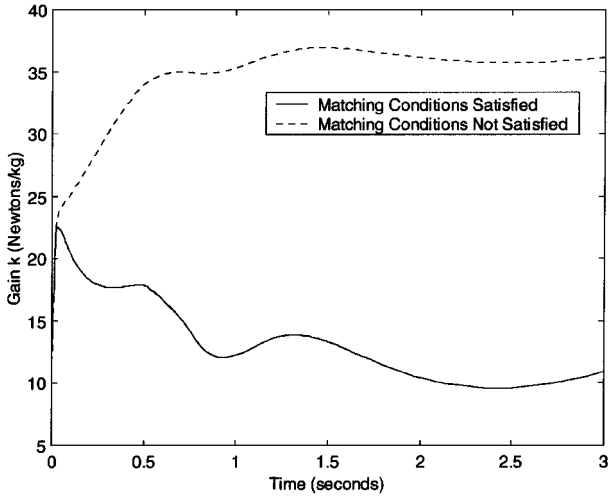

Fig. 11 Aerospace example, K vs time.

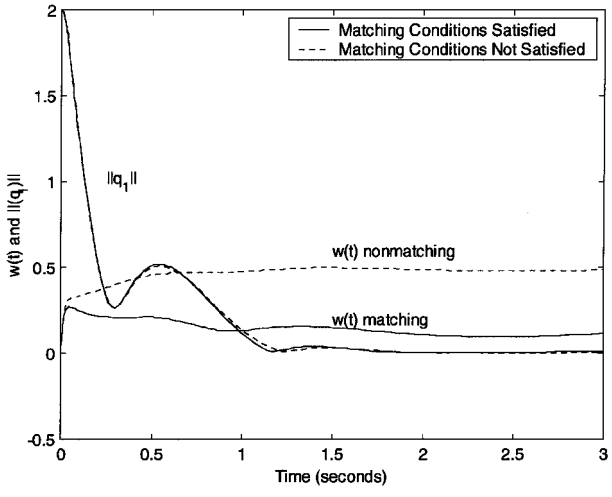

Fig. 12 Aerospace example, $\|q_1\|$ and $w(t)$ vs time.

and the dynamic responses are virtually identical. However, inspection of Fig. 11, which shows a plot of the gain K vs time, indicates that the gain for the nonmatching case is much larger than that of the matching case. Furthermore, Fig. 12 shows that it takes the matched case over 0.25 s longer for $w(t)$ to be greater than $\|q_1(t)\|$. This time could be reduced by increasing γ, but it would be at the expense more control effort, as shown in example 1. It should be noted that $S(t)$, which is not shown, is virtually identical for both cases.

Conclusions

A general sliding mode output feedback control algorithm applicable to a wide range of systems has been developed to guarantee robustness to bounded external disturbances and parametric uncertainty when there are more states than sensors. The robustness is achieved through proper selection of the gain vector associated with the nonlinear part of the sliding mode control law. It has extended previous work by including uncertainties to the control and A_{red} matrices. Details of an eigenvalue perturbation analysis for an uncertain matrix have been given. Simulation results have been presented for both matched and mismatched disturbances.

References

[1]Yallapragada, S. V., Heck, B. S., and Finner, J. D., "Reaching Conditions for Variable Structure Control with Output Feedback," *Journal of Guidance, Control, and Dynamics*, Vol. 19, No. 4, 1996, pp. 848–853.

[2]Wang, W.-J., and Fan, Y.-T., "New Output Feedback Design in Variable Structure Systems," *Journal of Guidance, Control, and Dynamics*, Vol. 17, No. 2, 1994, pp. 337–340.

[3]Kwan, C. M., "Sliding Control Using Output Feedback," *Journal of Guidance, Control, and Dynamics*, Vol. 19, No. 3, 1996, pp. 731–733.

[4]Lewis, A. S., Sinha, A., and Wang, K. W., "Sliding Mode Output Feedback Control of a Flexible Rotor via Magnetic Bearings," American Society of Mechanical Engineers, Paper 98-GT-407, June 1998.

[5]Lewis, A. S., and Sinha, A., "Sliding Mode Control of Mechanical Systems with Bounded Disturbances via Output Feedback," *Journal of Guidance, Control, and Dynamics*, Vol. 22, No. 2, 1999, pp. 235–240.

[6]Verghese, G. C., Fernandez, B. R., and Hedrick, J. C., "Stable Robust Tracking by Sliding Mode Control," *Systems and Control Letters*, Vol. 10, No. 1, 1988, pp. 27–34.

[7]Dorling, C. M., and Zinober, A. S. I., "Two Approaches to Hyperplane Design in Multivariable Variable Structure Control Systems," *International Journal of Control*, Vol. 44, No. 1, 1986, pp. 65–82.

[8]Wilkinson, J. H., *The Algebraic Eigenvalue Problem*, Oxford Univ. Press, Oxford, England, U.K., 1965, pp. 62–109.

[9]Smith, R. S., Chu, C.-C., and Fanson, J. L., "The Design of H_∞ Controllers for an Experimental Non-Collocated Flexible Structure Problem," *IEEE Transactions on Control Systems Technology*, Vol. 2, No. 2, 1994, pp. 101–109.

[10]Weigl, H. J., Paduano, J. D., and Bright, M. M., "Application of H_∞ Control with Eigenvalue Perturbations to Stabilize a Transonic Compressor," *Proceedings of the 1997 IEEE International Conference on Control Applications*, Inst. of Electrical and Electronics Engineers, New York, 1997, pp. 691–698.

[11]Smith, R. S., "Eigenvalue Perturbation Models for Robust Control," *IEEE Transactions on Automatic Control*, Vol. 40, No. 6, 1995, pp. 1063–1066.

[12]Slotine, J.-J. E., and Li, W., *Applied Nonlinear Control*, Prentice–Hall, Englewood Cliffs, NJ, 1991, pp. 276–307.

[13]Heck, B. S., and Ferri, A. A., "Application of Output Feedback to Variable Structure Systems," *Journal of Guidance, Control, and Dynamics*, Vol. 12, No. 6, 1989, pp. 932–935.